Vortex behavior near a spin vacancy in two-dimensional *XY* magnets

A. R. Pereira and L. A. S. Mól
Departamento de Física, Universidade Federal de Viçosa, 36571-000, Viçosa, Minas Gerais, Brazil

S. A. Leonel and P. Z. Coura
Departamento de Física ICE, Universidade Federal de Juiz de Fora, Juiz de Fora, CEP 36036-330, Minas Gerais, Brazil

B. V. Costa
Departamento de Física, ICEX, Universidade Federal de Minas Gerais, Caixa Postal 702, CEP 30123-970, Belo Horizonte, Minas Gerais, Brazil

(Received 9 July 2003; published 16 October 2003)

The dynamical behavior of anisotropic two-dimensional Heisenberg models is still a matter of controversy. In order to contribute to this discussion we use Monte Carlo and spin dynamics simulations as well as analytical calculations to study the behavior of vortices in the presence of nonmagnetic impurities. Our simulations show that vortices are attracted and trapped by the impurities. Using this result we show that if we suppose that vortices are not very much disturbed by the presence of the impurities, then they work as an attractive potential to the vortices explaining the observed behavior in our simulations.

DOI: 10.1103/PhysRevB.68.132409 PACS number(s): 75.30.Hx, 75.40.Mg, 75.10.Hk, 74.78.−w

The anisotropic Heisenberg model (AHM) in two dimensions has received a lot of attention recently. This is because of the fact that a large variety of models may be mapped in the AHM. It is an interesting model because it can support topological excitations, such as solitons and vortices, which are present in several important phenomena. Topological defects are present in condensed matter systems such as superconductors, liquid crystals, superfluids, magnetic materials, and several others. The knowledge of how such structures behave is essential for technological applications and an important condition for the understanding of many physical questions. Of great importance is the dynamical behavior of vortices in ordered structures. Knowing how vortices are pinned in superconductors is essential for applications such as magnetic levitation, improving magnetic resonance imaging devised for medical diagnosis, and many others. Topological defects can be the signature left behind by the cosmological phase transitions, which occur while the universe expands and cools. In addition to all of that, the study of the dynamics of the AHM model is interesting by itself. There are several questions that have not yet been addressed about the model. For example, the origin of the central peak in the dynamical structure factor observed in experiments and simulations is the source of several controversial interpretations. In fact, there is so far no theory that can fully explain the central peaks observed in simulations and experiments. A qualitative agreement is achieved by a phenomenological vortex gas theory, but one of its assumptions, namely, ballistic vortex motion,[1–3] is questionable.[4,5] Simulations have shown that a free vortex almost never travels more than one lattice spacing.[4,5] Of course, the existence of some kind of impurity in the system may affect the vortex motion and possibly the dynamical correlation function. For example, solitons near a nonmagnetic impurity in 2D antiferromagnets cause observable effects in EPR experiments.[6,7] Lattice defects such as impurities and dislocations play a crucial role in disrupting order in solids.

The main task of this paper is to consider the dynamical effects caused by impurities on topological defects. In this work we will consider the classical two-dimensional magnetic (*XY*) model, which is a special case of the anisotropic Heisenberg model, described by[8] $H=-J\Sigma_{m,n}(S_m^x S_n^x + S_m^y S_n^y)$. Here J is a coupling constant, S^α ($\alpha=x,y,z$) are the components of the classical spin vector $\vec{S}=(S^x,S^y,S^z)$, and the summation is over nearest neighbors in a square lattice. The spin field can be parametrized in terms of spherical angles as $\vec{S}=(\cos\theta\cos\phi,\cos\theta\sin\phi,\sin\theta)$, where we took $|\vec{S}|=1$. The continuum version of the *XY* Hamiltonian can be written as

$$H=\frac{J}{2}\int d^2r\left[\frac{m^2(\nabla m)^2}{1-m^2}+(1-m^2)(\nabla\phi)^2+\frac{4}{a^2}m^2\right], \quad (1)$$

where $m=\sin\theta$ and a is the lattice constant. The spin dynamics is given by the equations of motion $\dot{m}=\delta h/\delta\phi$, $\dot{\phi}=-\delta h/\delta m$, where h is the Hamiltonian density from Eq. (1). The introduction of nonmagnetic impurities modify the Hamiltonian in the following way.[9,10] As the model considers only spin interactions up to nearest neighbors, to take into account the presence of a nonmagnetic impurity we introduce a circular hole with radius of the order of the lattice spacing, inside of which the Hamiltonian density vanishes. The Hamiltonian (1) becomes[9]

$$H=\frac{J}{2}\int d^2r\left[\frac{m^2(\nabla m)^2}{1-m^2}+(1-m^2)(\nabla\phi)^2+\frac{4}{a^2}m^2\right]U(\vec{r}), \quad (2)$$

with $U(\vec{r})=1$ if $|\vec{r}-\vec{r}_0|\geqslant a$ and $U(\vec{r})=0$ if $|\vec{r}-\vec{r}_0|<a$, for a nonmagnetic impurity at $\vec{r}_0$. Early works[9,10] have found a repulsive force between the vortex and the nonmagnetic vacancy. The principal ingredient in the calculations was to suppose that the spin vacancy causes a small but global de-

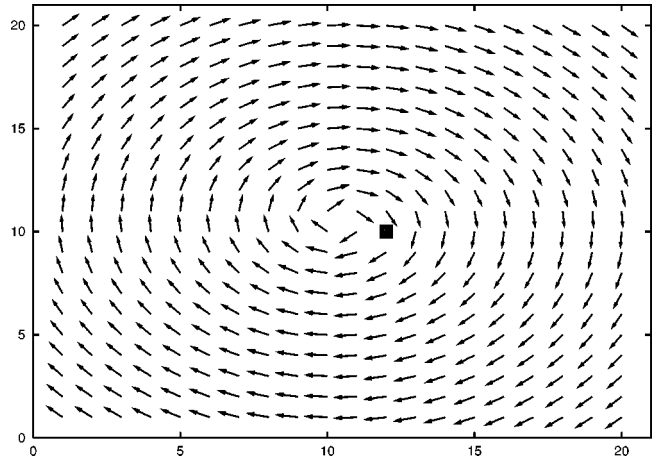

FIG. 1. A typical initial configuration. The square represents the spinless site.

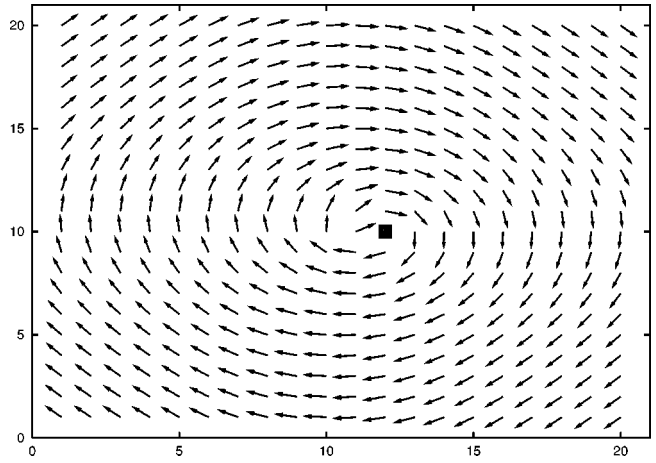

FIG. 2. Configuration after 70 time steps.

formation on the vortex structure. However, although the assumption of vortex deformation near the impurity seems reasonable, it needs a convincing demonstration. We discuss this question by means of numerical simulations, which will be used not only to check the validity of the approximations done, but also as a guide to give us a clue on which assumptions can be made in a safe way. We have performed spin dynamical simulations on a $L=20$ square lattice to observe the behavior of a single vortex initially located at the center of the system, in the presence of a spin vacancy located two sites away from the center of the system. In order to introduce a single vortex into the system, we have imposed diagonally antiperiodic boundary conditions[11]

$$\vec{S}_{L+1,y}=-\vec{S}_{1,L-y+1},\ \ \vec{S}_{0y}=-\vec{S}_{L,L-y+1},$$

$$\vec{S}_{x,L+1}=-\vec{S}_{L-x+1,1},\ \ \vec{S}_{x,0}=-\vec{S}_{L-x+1,L} \tag{3}$$

for all $1\leqslant x,y\leqslant L$. The discrete equation of motion for each spin is[12]

$$\frac{d\vec{S}_m}{dt}=\vec{S}_m\times\vec{H}_{ef}, \tag{4}$$

where

$$\vec{H}_{ef}=-J\sum_n\ (S_n^x\hat{e}_x+S_n^y\hat{e}_y) \tag{5}$$

and $\hat{e}_x$ and $\hat{e}_y$ are unit vectors in the x and y directions, respectively. The equations of motion were integrated numerically forward in time using a vectorized fourth-order Runge-Kutta scheme with a time step of $0.04J^{-1}$. The initial structure is shown in Fig. 1.

In contrast to the analytical results presented in Ref. 9, the simulation results show that the vortex structure does not change appreciably near the spin vacancy. The vortex center moves toward the spinless site, indicating an effective attractive potential of interaction between the vortex and the vacancy, as shown in Figs. 2 and 3. In Fig. 2 we show the configuration after 70 time steps and Fig. 3 after 150 time steps. We notice that after 150 time steps the position of the vortex center reaches the equilibrium with its center at the spinless site. The key point here is the property of nondeformation of the vortex configuration.

The attractive potential could also be obtained from our theoretical model Hamiltonian (2) by assuming that the vortex configuration is not deformed due to the presence of an impurity. Substituting both the nondeformed, static, and planar vortex solution $\phi_0=\arctan(y/x)$ located at the origin and a nonmagnetic impurity placed at the site $\vec{r}_0$ in Hamiltonian (2) we obtain

$$H_I=\frac{J}{2}\int\ (\nabla\phi_0)^2U(\vec{r})d^2x$$

$$=\frac{J}{2}\left[\int\ (\nabla\phi_0)^2d^2x-\int_{A(\vec{r}_0)}(\nabla\phi_0)^2dA(\vec{r}_0)\right], \tag{6}$$

where $A(\vec{r}_0)$ is the area of the hole with radius a around the point $\vec{r}_0$ that represents the spinless site. The integrals are easily calculated leading to

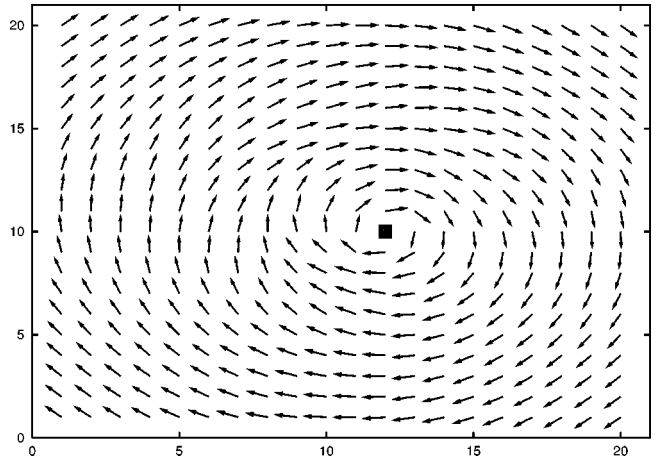

FIG. 3. Configuration after 150 time steps.

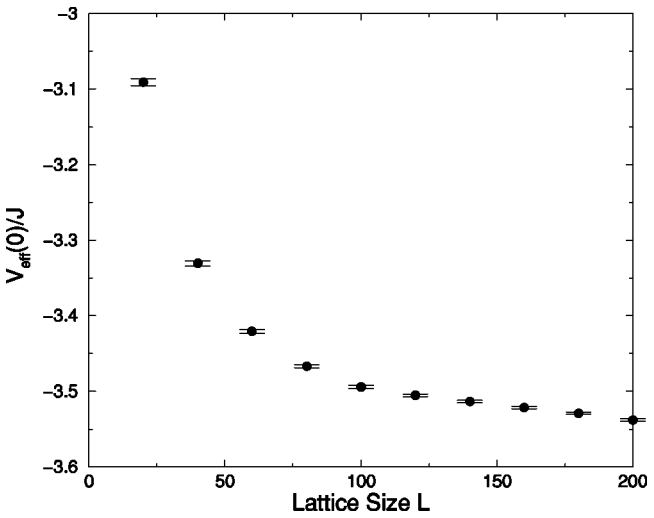

FIG. 4. Pinning energy $V_{\text{eff}}(0)/J$ for many sizes L of a square lattice. This energy tends to -3.54 J as L tends to infinity.

$$E_I = E_\nu + \frac{\pi J}{2}\ln\left(1-\frac{a^2}{r_0^2}\right), \tag{7}$$

where $E_I(\vec{r}_0)$ and $E_\nu = \pi J \ln(L/a_0)$ are the vortex energies in the presence and absence of the nonmagnetic impurity, respectively, for a system of size L. The constant[13] $a_0 = 0.24a$ present in E_ν, is some suitable short-distance cutoff to avoid spurious divergences due to the fact that the vortex center is a singularity in the continuum limit. Its appropriated value for the square lattice was determined numerically in Ref. 13. Of course, Eq. (7) is not valid in the limit $r_0 \to 0$, where the continuum approximation breaks down. In this limit there will have an intersection between the circular hole of the impurity and the structure of the vortex core. A point of the circumference of the impurity circle would meet the center of the vortex core lowering the vortex energy as $\vec{r}_0$ decreases. Then, from Eq. (7) the effective potential experienced by the two defects can be written as

$$V_{\text{eff}}(r_0) = E_I(r_0) - E_\nu = \frac{\pi J}{2}\ln\left(1-\frac{a^2}{r_0^2}\right), \quad \text{for } r_0 > a, \tag{8}$$

which is attractive. For large distances of separation ($r_0 \gg a$), Eq. (8) can be approximated by $V_{\text{eff}}(r_0) \approx -(\pi J a^2/2)(1/r_0^2)$. To know the behavior of the potential in the region inside the core ($r_0 \leqslant a$), we first put the hole exactly at the vortex center, obtaining $E_I = \pi J \ln(L/a)$, which leads to $V_{\text{eff}}(0) = E_I(0) - E_\nu = \pi J \ln(0.24) = -4.48$ J. We also calculate this pinning energy numerically for the case of zero temperature and for several square lattice sizes as can be seen in Fig. 4. Note that $V_{\text{eff}}(0)$ tends to -3.54 J in the thermodynamic limit. Using a different approach, Wysin[14] has found the approximated values -3.178, -1.937, and -5.174 J for square, hexagonal, and triangular lattices, respectively. We notice the reasonable agreement between the analytical result obtained using the continuum limit and the numerical results in a discrete lattice. Then, using the continuum approach, we modify Eq. (8) to get a complete function $V_{\text{eff}}(r_0)$, introducing a small constant b as follows:

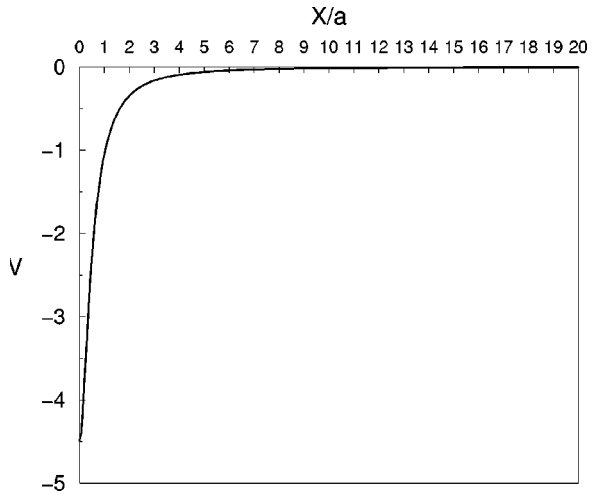

FIG. 5. Attractive potential as a function of X/a.

$$V_{\text{eff}}(r_0) = \frac{\pi J}{2}\ln\left(1-\frac{a^2}{r_0^2+b^2}\right), \tag{9}$$

with the condition

$$V_{\text{eff}}(0) = \frac{\pi J}{2}\ln\left(1-\frac{a^2}{b^2}\right) = \pi J \ln(0.24). \tag{10}$$

This artifact leads to an expression valid in all space that reproduces correctly the asymptotic limits for $b = 1.03a$. The potential [Eq. (9)] indicates that the vortex can be trapped by a nonmagnetic impurity. The attractive potential experienced by the vortex can be written as

$$V(X) = \frac{\pi J}{2}\ln\left(1-\frac{a^2}{X^2+b^2}\right), \tag{11}$$

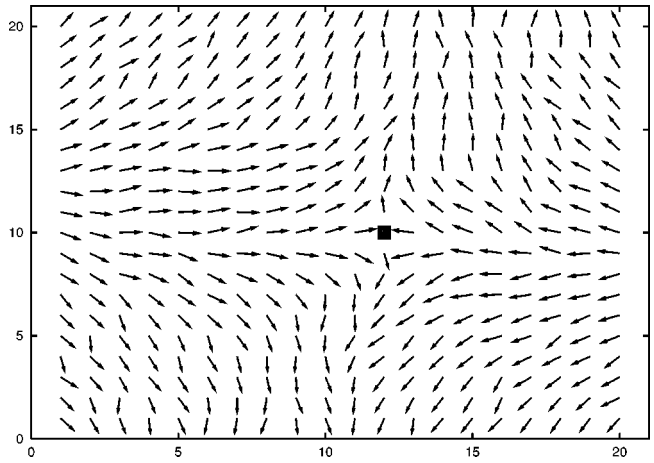

FIG. 6. Antivortex configuration after 2×10^5 MC steps. The impurity is located at site (12,10).

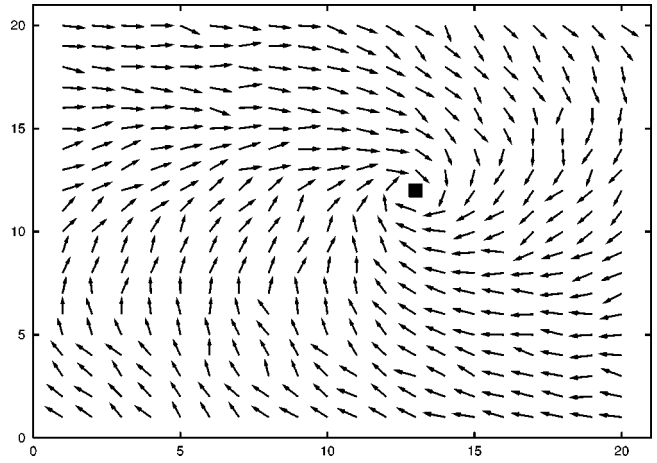

FIG. 7. Vortex configuration after 2×10^5 MC steps. The impurity is located at site (13,12).

where X is the distance between vortex center and the spinless site. It has a minimum at $X=0$ and goes to zero rapidly for $X>2a$ (see Fig. 5).

In order to observe the lowest energy configurations at low temperatures in a classical two-dimensional system described by the XY model with a nonmagnetic impurity, we performed Monte Carlo (MC) simulations. The simulations were done on $L=20$ square lattices at temperature $T=0.1$ in units of J/k_B (k_B is the Boltzmann constant), using a standard Metropolis algorithm[15] with diagonally antiperiodic boundary conditions [Eq. (3)] and random initial configurations. Using these boundary conditions, at low temperature, the equilibrium configurations can have a single vortex or a single antivortex. We have observed that after 10^5 MC steps the equilibrium configurations was reached. Figure 6 shows a single antivortex equilibrium configuration after 2×10^5 MC steps with the nonmagnetic impurity located at site (12,10). Figure 7 shows a single vortex equilibrium configuration after 2×10^5 MC steps with the nonmagnetic impurity located at site (13,12). We have observed that, in both cases, in the lowest energy configurations, the antivortex and vortex centers are located at the nonmagnetic impurity, which is in agreement with Eq. (11).

Of course, thermal fluctuations increases the system energy, but they should not affect the pinning energy, which is consequence of the pure magnetic interactions. Really, they may induce favorable energetic conditions for some vortices to escape from the vacancy.

In summary, using Monte Carlo and molecular dynamics simulations, we observed that a vortex structure put close to a nonmagnetic site in a square lattice does not appreciably change its geometry. As the system evolutes in time the vortex center moves toward the spinless site. By using a continuum approach we have modeled the interaction as an attractive potential which has a minimum for the vortex center located at spinless site, as observed in MC simulations. The study of the dynamics of diluted models can help us to understand the origin of the central peak found in early simulations. If the vortex motion is the important contribution, the presence of nonmagnetic sites will diminish the height of the central peak due to a trapping of vortices at that nonmagnetic sites.

This work was partially supported by CNPq and FAPEMIG (Brazilian agencies). Numerical work was done at the Laboratório de Computação e Simulação do Departamento de Física da UFJF.

[1] F.G. Mertens, A.R. Bishop, G.M. Wysin, and C. Kawabata, Phys. Rev. B **39**, 591 (1989).
[2] M.E. Gouvêa, G.M. Wysin, A.R. Bishop, and F.G. Mertens, Phys. Rev. B **39**, 11 840 (1989).
[3] A.R. Pereira, A.S.T. Pires, M.E. Gouvêa, and B.V. Costa, Z. Phys. B **89**, 109 (1992).
[4] J.E.R. Costa and B.V. Costa, Phys. Rev. B **54**, 994 (1996).
[5] B.V. Costa, J.E.R. Costa, and D.P. Landau, J. Appl. Phys. **81**, 5746 (1997).
[6] K. Subbaraman, C.E. Zaspel, and J.E. Drumheller, Phys. Rev. Lett. **80**, 2201 (1998).
[7] C.E. Zaspel, K. Drumheller, and K. Subbaraman, Phys. Status Solidi A **189**, 1029 (2002).
[8] J.M. Kosterlitz and D.J. Thouless, J. Phys. C **6**, 1181 (1973).
[9] L.A.S. Mól, A.R. Pereira, and A.S.T. Pires, Phys. Rev. B **66**, 052415 (2002).
[10] S.A. Leonel, P. Zimmermann Coura, A.R. Pereira, L.A.S. Mól, and B.V. Costa, Phys. Rev. B **67**, 104426 (2003).
[11] H. Kawamura and M. Kikuchi, Phys. Rev. B **47**, 1134 (1993).
[12] H.G. Evertz and D.P. Landau, Phys. Rev. B **54**, 12 302 (1996).
[13] G.M. Wysin, Phys. Rev. B **54**, 15 156 (1996).
[14] G.M. Wysin, cond-mat/0307448 (unpublished).
[15] N. Metropolis, A.W. Rosenbluth, M.N. Rosenbluth, A.H. Teller, and E. Teller, J. Chem. Phys. **21**, 1087 (1953) and for a review, see, e.g., *Monte Carlo Methods in Statistical Physics*, edited by K. Binder (Springer, New York, 1979).